iScience

Article

Emergent network properties link phenotypic modules to ecomorphological divergence in carnivoran mammals

Graphical abstract

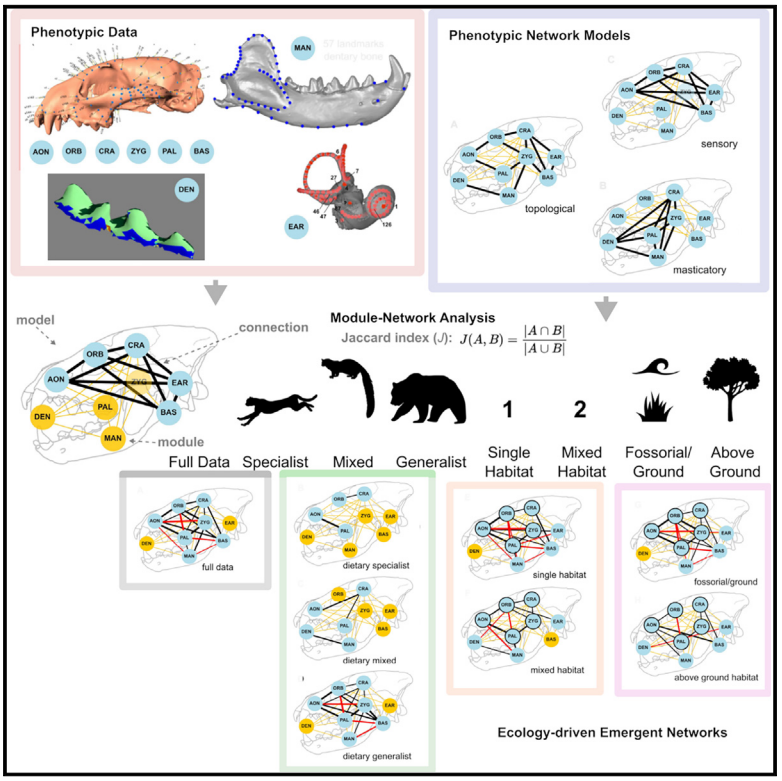

Highlights

- Common modules related to development and function are present in mammal skulls
- The modules form a topological network, where connectivity is spatially organized
- Deviations from this general pattern are linked to evolutionary convergence
- Macroevolutionarily recombined functional networks reflect ecological adaptations

Authors

Z. Jack Tseng (曾志傑), Camille Grohé, Bailee DesRocher, Emily Waldman, John J. Flynn

Correspondence

zjt@berkeley.edu

In brief

Animal morphology; Biological morphology; Network modeling; Zoology

Tseng et al., 2025, iScience *28*, 111828
February 21, 2025
https://doi.org/10.1016/j.isci.2025.111828

CellPress

iScience

CellPress
OPEN ACCESS

Article

Emergent network properties link phenotypic modules to ecomorphological divergence in carnivoran mammals

Z. Jack Tseng (曾志傑),[1,2,7,*] Camille Grohé,[2,3] Bailee DesRocher,[4] Emily Waldman,[5] and John J. Flynn[2,6]
[1]Department of Integrative Biology and Museum of Paleontology, University of California, Berkeley, Berkeley, CA 94720, USA
[2]Division of Paleontology, American Museum of Natural History, New York, NY 10024, USA
[3]Laboratoire Paléontologie Évolution Paléoécosystèmes Paléoprimatologie (PALEVOPRIM), UMR 7262, CNRS & Université de Poitiers, 86000 Poitiers, France
[4]Beautiful Critters Science Illustration and Motion Design, Los Angeles, CA, USA
[5]School of Dental Medicine, University at Buffalo, Buffalo, NY 14215, USA
[6]Richard Gilder Graduate School, American Museum of Natural History, New York, NY 10024, USA
[7]Lead contact
*Correspondence: zjt@berkeley.edu
https://doi.org/10.1016/j.isci.2025.111828

SUMMARY

The skull is the skeletal core of a multicomponent, multifunctional system that controls organismal activities. A common set of skeletal modules is known in mammal skulls and is correlated to developmental and functional compartmentalization. However, it is unclear to what extent these modules further organize into, and evolve as, higher-level networks. Here, we show that mammalian skull modules represent a topological network, where inter-module connectivity correlates with spatial proximity. Deviations from this general pattern are linked to evolutionary convergence. Terrestrial and aquatic species show accelerated sensory and masticatory module evolution and reduced network linkages compared to above ground species. Extreme feeding ecologies show accelerated sensory and masticatory module evolution yet dissimilar networks. Despite common topological network-like organization of skull elements, macroevolutionary recombination can generate functional networks that link significantly to ecological adaptations. More generally, mammal skull elements exhibit emergent network properties as multi-dimensional form-function linkages on which evolution may act.

INTRODUCTION

The vertebrate head is a composite structure that represents the integration of tissues from different developmental (dermal versus neurocranial) and embryological (pharyngeal arch) origins. The ossified scaffolding of the head, the skull (cranium and mandible), reflects these varied tissue origins in the arrangement, shape, and size of its constituent bones.[1] The skull in mammals is a further specialized structure that represents the only part of the skeleton that simultaneously contains an arrangement of bones characterized by joints, sutures, and both partial and total fusion of elements. On top of these salient anatomical and developmental characteristics, skulls serve a vital role in housing and controlling sensory, masticatory, and communicatory systems. Much research has assessed the effects of evolutionary specialization of one of more of these systems on the diversity of skull shapes and structures during the Cenozoic radiation of mammals, but few studies have assessed their interaction influences of skull morphology.[2]

A prevailing paradigm that has begun to unify research on the evolutionary morphological consequences of heterochrony,[3] developmental canalization,[4] and functional specialization in the mammalian skull is the establishment of major phenotypic trait clusters that persist across mammal clades.[5] The clustered distribution of phenotypic covariation among skull regions, and the degree to which the units of covarying structures (called modules) vary relative to other modules, both influence the tempo and mode of skull evolution in mammals. These research efforts have revealed a set of six skull phenotypic units of measure on which natural selection likely operates: the anterior oral-nasal, basicranium, molar/dentition, cranial vault, orbit, and zygomatic-pterygoid regions.[5,6]

Despite advances in understanding these primary or first-order mammalian skull modules, there have been few insights into complexities that develop from higher-order interactions among first-order modules. One possible consequence of such interactions may be a further canalization of evolutionary pathways for skull morphology into higher-level networks of phenotypic modules, or second-order networks (emerging sets or clusters of primary modules composed of first-order modules that are developmentally and functionally defined). Such emergent patterns reflecting differential covariation of skull structures

may in turn associate with different adaptive evolutionary pathways. Although modular pathways of change have been clearly documented in the mammal skull,[5,7] how the modules interact to facilitate or constrain the development and variation of one another cannot be easily studied by using the pairwise comparisons currently employed in the literature. An organism's ecological role in their biological communities also is where the "rubber meets the road" in terms of how phenotype relates to life history and ecological traits that determine fitness. Specifically, it is unknown whether the interactions among known skull modules across all of Mammalia constitute emergent properties sensitive to ecological conditions (e.g., habitat, food resources, abiotic factors, etc.) that may enhance or limit skull shape diversification over macroevolutionary timescales.

Relevant to these questions of the nature and role of phenotypic module evolvability in ecological divergence and specialization, we know that there can be elevated covariation in morphological structures in hypercarnivorous mammals compared to generalists.[8] Furthermore, topologically, articulated structures such as the cranium and mandible can still show decoupled modes of evolution.[9] What we do not yet know is whether currently identified first-order skull phenotypic modules exhibit higher-order covariation patterns and evolutionary rates that further reflect ecological adaptations.

We should reasonably expect that complex anatomical systems such as skulls vary not only in pairwise comparisons, as in prior examinations of phenotypic modules, but also in emergent properties such as connectivity and higher-level modularity. As far as we are aware, no systems approach has been taken to investigate the presence of such phenotypic complexity in the skeleton. Here, we present a new quantitative framework, using principles of network analysis, to assess the degree to which mammalian skull phenotypic module networks could be "rewired" or recombined under different ecological specializations. We use carnivoran mammals as a study system to test two major sets of hypotheses.

(1) First, we assess whether morphological shape covariation and evolutionary tempo patterns can be explained by functional systems: our null hypothesis is that patterns of morphological shape covariation and evolutionary tempo in different regions of the skull simply follow topological proximity or relationships. In other words, higher degrees of correlation are expected for adjacent morphological modules than modules indirectly associated through a topologically intervening morphological unit (Figure 1A). In addition to this topological null model, we also define and test two alternative models: a masticatory function and a sensory function integration model, respectively (Figures 1B and 1C). A sensory integration model predicts higher correlation among skull modules housing sensory organs; a masticatory integration model predicts higher correlation among skull modules involved in jaw-closing muscle attachment and/or housing the dentition.
(2) Second, we ask whether morphological shape covariation and evolutionary tempo patterns can be explained by ecology: our null hypothesis is that taxa exhibiting different ecological characteristics in dietary breadth, habitat breadth, and terrestriality do not differ in the patterns of skull module covariation. This hypothesis is evaluated both by (1) testing for significance of morphological integration and evolutionary rate covariation with no *a priori* modules defined, and (2) testing for higher covariation of shape traits and evolutionary rates in modules defined in the topological, sensory, and masticatory models above, respectively, compared to morphological regions not included in those three models.

RESULTS

Patterns of phylogenetic integration

In the all-data partition analysis of phylogenetic integration among first-order morphological modules, 18 of 36 (50%) comparisons (the number of pairwise comparisons for k partitions is "k(k-1)/2", which for k = 9 comes to 36 comparisons) returned statistically significant integration values. Dietary breadth 1 (specialist) and 3 (mixed diet) partition categories each returned 2/36 comparisons with significant integration. Dietary breadth 6 (generalist) exhibited 16/36 significant integration pairings. Habitat breadth 1 contained 17/36 significant integrations, and habitat 2 showed 12/36. In terrestriality categories, terrestrial taxa showed the highest number of integrated pairings (11/36), followed by above ground dwelling taxa (8/36), then semi-aquatic/aquatic taxa (6/36) (Table S1).

Phenotypic module network model fit

The covariation patterns among phenotypic modules in the full dataset (the baseline carnivoran model; Figure 2) are most consistent with a topological model of morphological integration (Figure 3A; Tables 1 and 2). The full dataset best fits the topological model, with a Jaccard index of 0.67 (Figure 4), but the similarity is not statistically significant ($p = 0.08$) (Table 2). Among the dietary breadth categories, dietary specialists best and significantly fit a topological network model, with a Jaccard similarity index of 0.17 ($p = 0.05$). Taxa with mixed dietary breadth best fits a masticatory network model, but the similarity is not statistically significant (J = 0.20, $p = 0.11$). Dietary generalists are best characterized by a network model similar to the baseline all-Carnivora model (J = 0.83, $p = 0.0001$) and secondarily a topological network model (J = 0.67, $p = 0.04$); both model similarities are statistically significant.

In habitat breadth, those species living in a single habitat best fit an all-Carnivora network model (J = 0.72, $p = 0.01$) whereas species in mixed habitats best fit a topological model (J = 0.58, $p = 0.0027$). In the terrestriality trait, the terrestrial + water-associated species best fit a baseline carnivoran model (J = 0.78, $p = 0.0004$) and secondarily the topological network model (J = 0.67, $p = 0.04$). Lastly, the above ground species best fit the baseline carnivoran model (J = 0.44, $p = 0.0013$) (Table 2; Figure 4). Each of these model fits is statistically significant. In sensitivity analyses where terrestrial and water-associated taxa were separated into distinct categories, the terrestrial species best fit a baseline carnivoran model (J = 0.55, $p = 0.0001$),

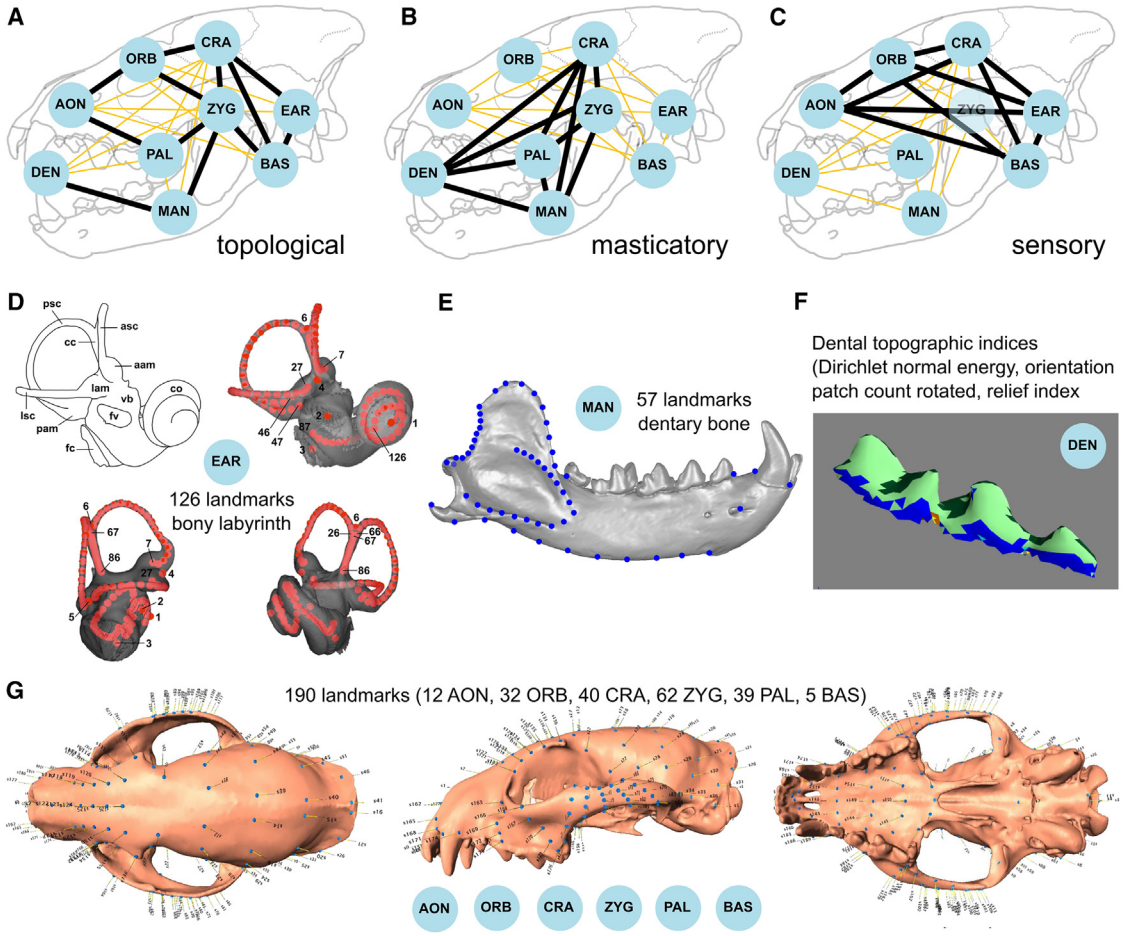

Figure 1. Network models proposed and datasets tested in this study

(A) Topological network model.
(B) Masticatory network model.
(C) Sensory network model.
(D) Bony labyrinth landmarks for the ear dataset.
(E) Mandibular landmarks for the mandible dataset.
(F) Dental topographic indices for the dentition dataset.
(G) Cranial landmarks and their all-mammal phenotypic module divisions analyzed. Abbreviations: BAS: basicranium, CRA: cranial vault, DEN: dentition, EAR: bony labyrinth, ORB: orbit, MAN: mandible, AON: anterior oral-nasal, PAL: palatine, ZYG: zygomatic-pterygoid region.

whereas water-associated species fit a topological model (J = 0.42, p = 0.0034); both are significant fits based on a criterion of p = 0.05.

Phenotypic module network evolutionary rates

Analysis of evolutionary rates by ecological trait categories indicates that: (1) the rates of sensory module (p = 0.037) and masticatory module (p = 0.036) evolution in species with mixed dietary breadth are significantly lower than evolutionary rates in dietary specialist and dietary generalist groups, (2) All module evolutionary rates are significantly slower in above ground taxa than all other (non-above ground dwelling) taxa (p = 0.01 to 0.03), and (3) the ear (p = 0.024) and dentition (p = 0.04) modules exhibit similar significant evolutionary rate decreases in above ground taxa (i.e., acceleration of evolutionary rate in terrestrial and semi-aquatic/aquatic taxa) (Table 3).

Phenotypic module networks across ecological partitions

There are no network connections common to all ecological categories (dietary breadth, habitat breadth, and terrestriality). Furthermore, there are no network connections in common among dietary breadth categories. Although the habitat breadth and terrestriality categories do not share a common set of best fit network models, all four ecological groups (single habitat, mixed habitat, non-above ground taxa, and above ground taxa) share a core sub-network composed of the anterior oral-nasal, orbit, palatine, zygomatic-pterygoid, and cranial vault modules (Figures 3E–3H).

Sampling power

A Levene's test between the empirical dataset and the simulated dataset yielded a p value of 0.0043, indicating that the variance in

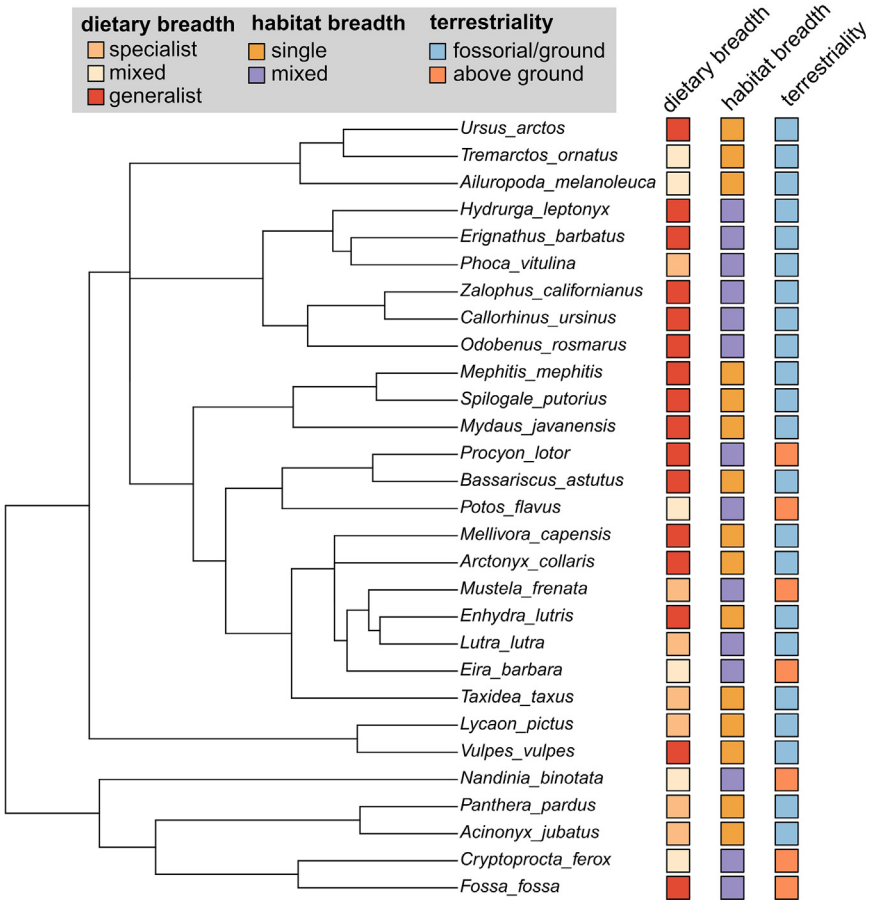

Figure 2. Phylogeny of Carnivora taxa included in the analyses

Ecological traits and coded categories indicated to the right of taxon names. Data for the phylogeny extracted from timetree.org; data for the ecological traits extracted from the PanTHERIA database.

Jaccard similarity distributions is significantly different between the datasets. The empirical dataset contains two main clusters of Jaccard similarity values: those with J $\sim$ 0.7 and another with J $\sim$ 0.15 (Figure 6A). In contrast, the randomly resampled simulated dataset exhibits a continuous distribution of second-order networks that span the range of J values observed in the empirical dataset.

DISCUSSION

A common set of skull phenotypic modules had been found previously across mammal clades.[5,6] The ancestral presence of those mammalian modules imposes initial conditions on how variation at the phenotypic level is generated and maintained on macroevolutionary timescales. We applied the first network analytical approach to capture the complexity of multi-level modularity patterns in the mammal skull and found that dietary and locomotor ecologies significantly "rewire" the baseline network of phenotypic modules observed in carnivorans. The emergent higher-order modular properties of phenotypic regions that were already individually modular (first-order covariances) provide new scenarios in which selection could act differently on first-order modularity versus on evolutionary patterns in second-order module networks (Figure 5).

Contrary to the generally assumed importance of sensory and feeding/masticatory selective pressures in driving mammalian skull evolution, we did not observe a significant sensory or masticatory modularity network component (which we defined *a priori*) associated with dietary breadth, habitat breadth, or terrestriality measures of dietary and locomotor ecology (Table 2). Instead, a topological module network of closer associations among spatially adjacent modules was a better fit. On the other hand, rates of phenotypic evolution are substantially and significantly correlated with skull regions involved in sensory and masticatory function, with mixed diet and above ground dwelling species exhibiting significantly lower evolutionary rates than other ecologies (Table 3). These findings outline dual pathways for ecological specialization: one that can occur via second-order reorganization of first-order phenotypic modules, and the other through varying the tempo of evolution of both first-order and second-order phenotypic networks within the skull. It is important to note that the broad ecological categorizations adopted from the PanTHERIA database provide only a general framework for mammals, but there might exist differential second-order modularity networks *within* finer partitions of the categories (e.g., narrow dietary breadth may include vertebrate tissue specialists and plant specialists, which likely have distinct form-function relationships with cranial network elements) that are masked by these broad, general categorizations. Future analyses could benefit from further examination of finer partitions within the ecological categories or incorporation of quantitative ecological trait models.[10]

The quantity of second-order modules in the carnivoran skull appears to vary independently from either rate-driven or network-driven shifts in skull modularity associated with different ecologies. Above ground dwelling species exhibit a phenotypic network with low evolutionary rates across all first order traits analyzed (Table 3) but evolved a high degree of second-order integration (i.e., the network is characterized by a single module wherein all first-order modules are connected to at least one other module; Figures 3 and 4). In contrast, mixed feeders also exhibit low evolutionary rates which are coupled with low degree of second-order integration (the network is characterized by six first-order modules; Figures 3 and 4). This decoupling of skull

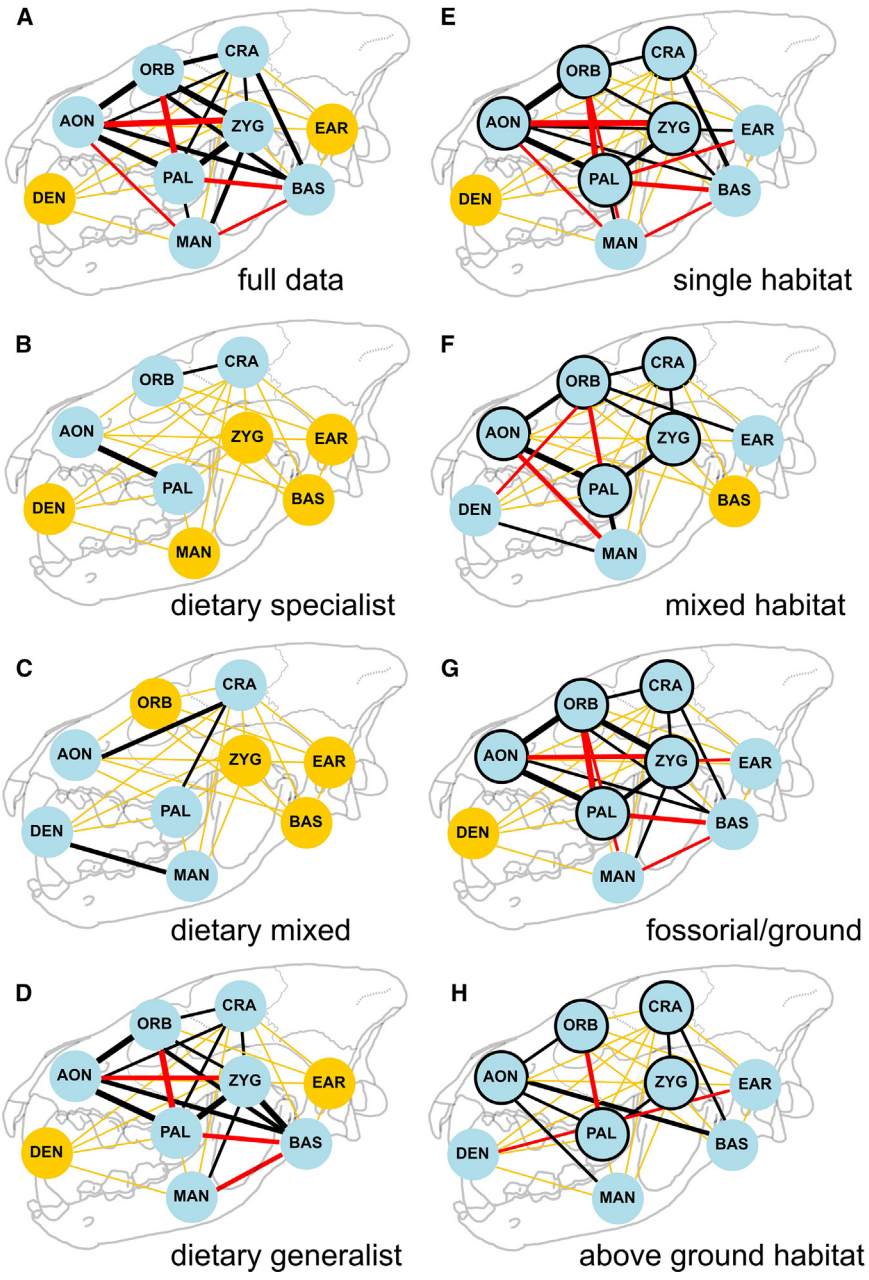

Figure 3. Network graphs showing module integration in full and ecological data partitions

Network plots were generated from results of phylogenetic integration tests separately for (A) full dataset, (B) dietary specialist group, (C) mixed diet group, (D) dietary generalist group, (E) single habitat, (F) mixed habitat, (G) non-above ground dwelling group, and (H) above ground dwelling group. Color coding—black lines: network connections expected from *a priori* network models; red lines: network connections absent in predicted models; blue circle infill: phenotypic modules forming connected networks; yellow circle infill: phenotypic modules that do not co-vary with others. Black outlines encircling modules indicate core subset-network modules found across the habitat breadth and terrestriality groups (AON [anterior oral-nasal], CRA [cranial vault], ORB [orbit], PAL [palatine], ZYG [zygomatic-pterygoid region). Network connection line thickness is proportional to the strength of the phylogenetic integration result.

modularity network complexity and evolutionary rate magnitude in Carnivora echoes previous findings in other vertebrates,[11] and similarly could have served as another source of a wide array of possible combinatorial evolutionary outcomes in module linkages and skull morphologies, and therefore is a possible mechanism to overcome constraints derived from first-order phenotypic canalization observed within the Mammalia-wide modules.[5]

Several ecological categories that exemplify major transformations observed repeatedly in vertebrates show relatively higher evolutionary rates of second-order networks. Terrestrial and semi-aquatic/aquatic species exhibit less integrated second-order networks overall, but more intra-network connections than above ground taxa. This marked difference in network integration is associated with elevated evolutionary rates of skull shape in terrestrial and semi-aquatic/aquatic taxa, suggesting that a less integrated network can permit higher evolutionary rates and possibly a greater number of "mix and match" phenotypic configurations. These findings suggest second-order phenotypic networks play a role in morphological evolution during major macroevolutionary transitions to open environments or secondary aquatic adaptations.[12] Within dietary breadth categories, specialists exhibit relatively elevated evolutionary rates with a high degree of second-order modularity. We propose that this indicates an increase in the number of possible evolutionary configurations of individual first-order skull modules can lead to unexpectedly more rapid evolution in the covarying modules comprising the second-order networks in specialists. Given recent findings that high biting velocity in Carnivora can be associated with diverse skull morphologies, whereas high bite force cannot,[13] second-order modularity differences may serve more generally as an important evolutionary mechanism underlying differential form-function linkages in many distinct functional traits in carnivoran and other mammals.

The finding that ecological specialists exhibit higher second-order modularity rather than more integrated craniodental systems is consistent with previous findings in carnivorans,[14] shrews,[15] and bats.[16,17] Evidence in this study and others

Table 1. *A priori* network models tested in the study

	BAS	CRA	DEN	EAR	ORB	MAN	AON	PAL
*Topological Model								
CRA	+	–	–	–	–	–	–	–
DEN	–	–	–	–	–	–	–	–
EAR	+	+	–	–	–	–	–	–
ORB	–	+	–	–	–	–	–	–
MAN	–	–	+	–	–	–	–	–
AON	–	–	–	–	+	–	–	–
PAL	–	–	–	–	–	–	+	–
ZYG	+	+	–	–	+	+	–	+
*Masticatory Model								
CRA	–	–	–	–	–	–	–	–
DEN	–	+	–	–	–	–	–	–
EAR	–	–	–	–	–	–	–	–
ORB	–	–	–	–	–	–	–	–
MAN	–	+	+	–	–	–	–	–
AON	–	–	–	–	–	–	–	–
PAL	–	+	+	–	–	+	–	–
ZYG	–	+	+	–	–	+	–	+
*Sensory Model								
CRA	+	–	–	–	–	–	–	–
DEN	–	–	–	–	–	–	–	–
EAR	+	+	–	–	–	–	–	–
ORB	+	+	–	+	–	–	–	–
MAN	–	–	–	–	–	–	–	–
AON	+	+	–	+	+	–	–	–
PAL	–	–	–	–	–	–	–	–
ZYG	–	–	–	–	–	–	–	–

A plus sign indicates predicted network link presence. BAS: basicranium, CRA: cranial vault, DEN: dentition, EAR: bony labyrinth, ORB: orbit, MAN: mandible, AON: anterior oral-nasal, PAL: palatine, ZYG: zygomatic-pterygoid region.

suggest that morphofunctional specialization appears as one or more peaks in the context of a performance landscape for phenotypic traits.[18–20] Rather than integrating skull regions into a specialized system that evolves faster but in fewer directions, ecomorphological specialization to different adaptive peaks may be associated with different functional demands that are reflected in low overall second-order modularity when specialists are considered as a group relative to generalists. This raises a fascinating possibility that macroevolutionary shifts under second-order modularity network controlled morphological variation may traverse the adaptive landscape in a punctuated manner rather than a smooth one. In other words, a continuum of adaptive peaks and valleys conceptualized in a microevolutionary framework may not readily translate into macroevolutionary contexts. Presence of second-order modularity instead could facilitate non-gradual shifts that appear as more punctuated bursts of change in morphofunctional traits.[21]

From a developmental perspective, first-order morphological modules that seldom participate in the second-order networks identified in this study seem to represent multiple embryological origins. On the other hand, the core of the second-order network modules represents bony elements that largely are of a single developmental origin, the dermatocranium. Of the eight second-order networks characterized in this study (Figure 3), dental topographic traits participate in the least number of networks and the dentition represents a tissue restricted to the first pharyngeal arch in mammals. The second least integrated structure, the inner ear (bony labyrinth), forms as otic placodes originated in but distinct from the ectoderm. The third least integrated partition, the basicranial region, originates from the neurocranium. These broad embryological associations suggest that an overlay in variability and evolvability of hard tissues with varying embryological origins and secondary ossification centers may be reflected in, or even responsible for, the interplay between first-order and second-order network properties observed in this study. Koyabu et al.[3] demonstrated the presence of embryological modularity and control in mammalian cranial ossification and encephalization, pointing to the possibility that simultaneous selective demands from sensory, biomechanical, and other functions served by the skull are able to modify developmental and ossification patterns to generate the second-order network patterns studied herein.

Future research covering greater taxonomic breadth is necessary to more fully test the outcomes of finer combinations of ecological characteristics (e.g., how taxa with specific habitat-diet combinations may exhibit unique second-order module linkage networks different from those characterized independently for the broad across-Carnivora analysis of habitat versus diet) and the possibility that additional decoupling of tempo and mode of phenotypic network evolution could be identified within those specific combinations. The consideration of trait interactions across dietary, locomotor, and other ecological traits would permit assessment of the effect of simultaneous or competing functional demands

Table 2. Bootstrap test *p* values of computed Jaccard similarity indices

	Full data	Specialist	Mixed	Generalist	Single habitat	Mixed habitat	Fossorial/Ground	Above-ground
Full data/Baseline	–	0.15	0.46	**0.0001**	**0.01**	0.06	**0.0004**	**0.0013**
Sensory model	0.33	0.53	0.87	0.70	0.69	0.90	0.70	0.67
Masticatory model	0.85	0.42	0.11	0.76	0.10	0.90	0.32	0.24
Topological model	0.08	**0.05**	0.94	**0.04**	0.63	**0.0027**	**0.04**	0.39

Results show goodness of fit between the four *a priori* network models and network models computed from phenotypic data by ecological categories (dietary breadth, habitat breadth, and terrestriality). Model fits that are statistically significant at the $p \leq 0.05$ level indicated in bold font.

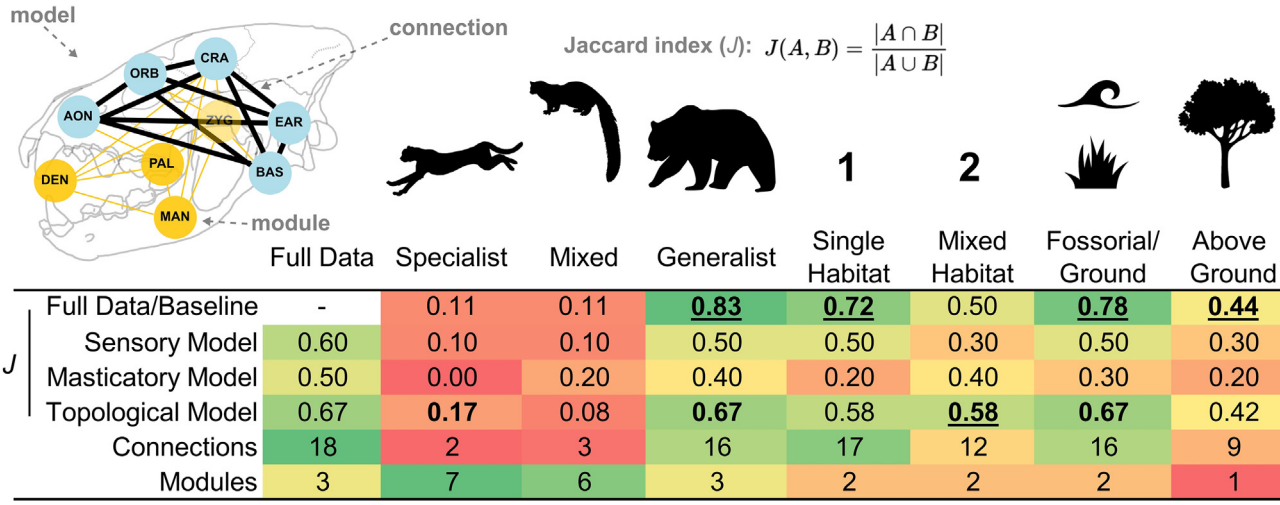

J		Full Data	Specialist	Mixed	Generalist	Single Habitat	Mixed Habitat	Fossorial/ Ground	Above Ground
	Full Data/Baseline	-	0.11	0.11	**0.83**	**0.72**	0.50	**0.78**	**0.44**
	Sensory Model	0.60	0.10	0.10	0.50	0.50	0.30	0.50	0.30
	Masticatory Model	0.50	0.00	0.20	0.40	0.20	0.40	0.30	0.20
	Topological Model	0.67	**0.17**	0.08	**0.67**	0.58	**0.58**	**0.67**	0.42
	Connections	18	2	3	16	17	12	16	9
	Modules	3	7	6	3	2	2	2	1

Figure 4. Phenotypic network model testing by ecological category

Heatmap colors in cells indicate level of network similarity (J, Jaccard index) or number of connections/modules in each of the four fitted network models (*post hoc* full data module network—Figure 3A and *a priori* functional networks—Figures 1A–1C). Jaccard indices significant at the $p = 0.05$ level in bold font; those significant at the $p = 0.01$ level also are underlined (p values reported in Table 2). Heatmap colors indicate data values along a spectrum from minimum (red) to maximum (green) values for modules (from 1 to 7), connections (from 2 to 18), and Jaccard index (from 0 to 0.83).

acting in multiple ecological dimensions on evolvability and clade longevity. Furthermore, our results highlight a novel determination of the presence of different second-order networks in specialists versus generalists. We propose that it also illuminates the important potential for a new network-driven, multi-level module mechanism that drives evolution, and which can be quantitatively evaluated using our new approach. A fertile testing ground for this approach would be to re-examine classic examples of the macroevolutionary ratchet, whereby lineages with more specialized morphology or ecology exhibit reduced ability to change evolutionary trajectories, using this second-order modularity network framework. Future efforts employing this new framework can continue to unravel the role of intrinsically determined extinction pathways and how they interact with broader environmental events on geologic timescales.

Given the relatively small taxonomic sampling breadth (29 extant carnivoran species), we advise caution in interpretation of the network module results. We intentionally sampled as broadly and evenly across the range of ecological traits tested as possible within the 29 species, but in some cases the small number of samples within ecological categories (e.g., sampling only six species with mixed dietary breadth) may limit the statistical support of the second-order network modules identified using our proposed approach. Although our simulation analyses indicate that the network modules observed are significantly more variable and clustered in their dissimilarity to each other than in simulated datasets, the degree of network similarity (as measured by the Jaccard index) does overlap between empirical and simulated datasets (Figure 6). The higher variance and clustering of empirical data both point to the presence of non-random second-order module networks that may reflect distinctive evolutionary histories associated with different ecological morphologies. Future studies should expand both the ecological and taxonomic breadth in order to fully

Table 3. Evolutionary rate comparisons in *a priori* and *post hoc* phenotypic network modules

Phenotypic network module	Dietary breadth	Habitat breadth	Terrestriality
Sensory	$p = 0.037$; specialist and generalist higher	n.s.	$p = 0.0125$; terrestrial/aquatic higher
Non-sensory	n.s.	n.s.	$p = 0.032$; terrestrial/aquatic higher
Masticatory	$p = 0.036$; specialist and generalist higher	n.s.	$p = 0.0105$; terrestrial/aquatic higher
Non-masticatory	n.s.	n.s.	$p = 0.015$; terrestrial/aquatic higher
Core habitat/terrestriality	–	n.s.	$p = 0.009$; terrestrial/aquatic higher
Ears	–	n.s.	$p = 0.024$; terrestrial/aquatic higher
Dentition	–	n.s.	$p = 0.04$; terrestrial/aquatic higher
Mandible	–	n.s.	n.s.

Statistically significant differences in evolutionary rates listed with p values from permutation tests. N.s., non-significant.

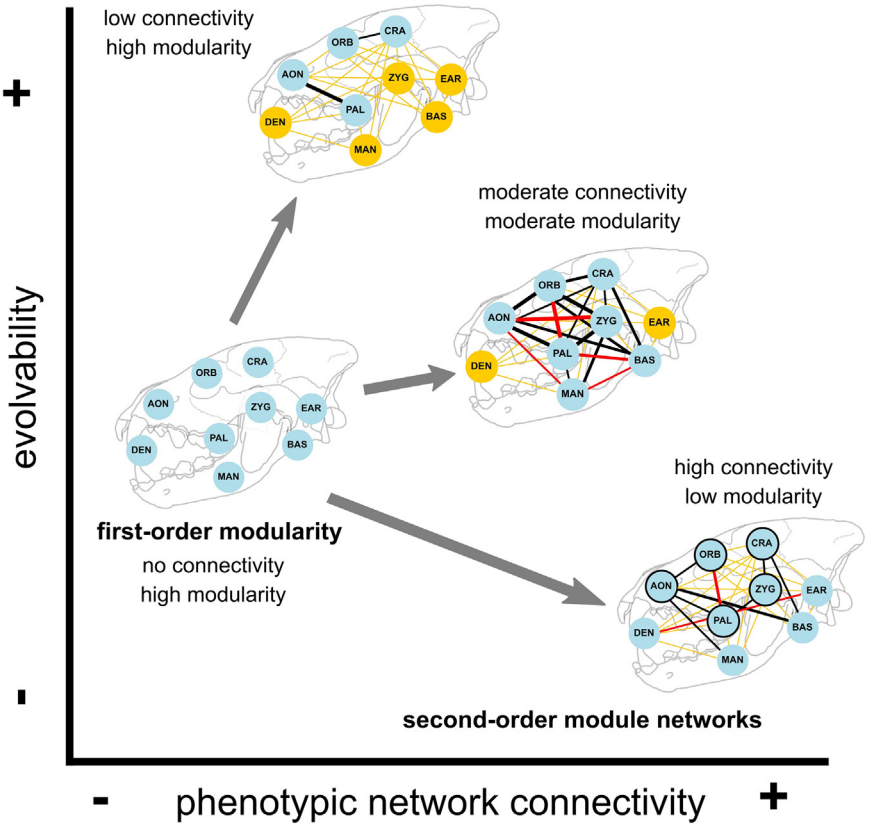

Figure 5. Proposed framework for future research agenda on multi-level modularity patterns

The common phenotypic modules found in all mammals[5,6] represent first-order modularity data that do not capture emergent properties of network-like rewiring of trait covariation evident in second-order module network analyses performed in this study. Evolvability is hypothesized to be related to the degree to which second-order module networks are connected (i.e., the degrees of phenotypic variational freedom and thus potential for evolutionary change should be proportional to the connectivity of second-order networks).

understand the significance of the network modules identified in our study system.

In summary, our skull module network analyses demonstrate that first-order skull phenotypic modules common to nearly all mammals are "rewirable" as more complex, second-order interaction networks of multiple covarying modules that correspond with dietary and locomotory ecological specializations. In a carnivoran model system we determined that terrestrial and water-associated lifestyles accelerated bony labyrinth evolution, and more generally also accelerated sensory module evolutionary rates. In contrast, those taxa with mixed dietary breadth relative to specialist and generalist taxa resulted in slower sensory module evolution, and dietary specialization is more generally associated with breakdown of the baseline second-order phenotypic module network common to carnivorans. Our analyses document for the first time that (1) second-order network reorganization can occur despite first-order phenotypic modularity constraints, and (2) decoupling of network connectivity and evolutionary rates together offer promising new mechanisms to explain patterns of phenotypic evolution and ecological adaptation. Both findings indicate that, from a common or ancestral modularity blueprint in mammals, new skull form-function relationships are discovered as previously unexpected emergent properties when analyzed in a network-based paradigm.

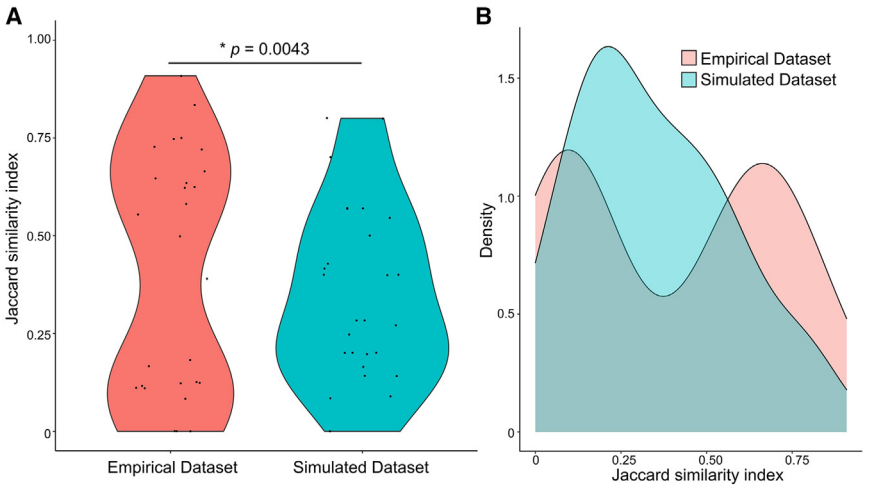

Figure 6. Jaccard similarity distributions in empirical versus randomly-generated simulated datasets

(A) Boxplot.

(B) Density plot. *p* value calculated using Levene's test of homogeneity of variance.

Limitations of the study

The emergent network properties identified in this study are based on a carnivoran study system; additional analyses of other mammalian species data are necessary to confirm any Mammalia-wide skull module network configurations. Additionally, only male specimens were used in order to standardize the sex of specimens in the analyses; different degrees of sexual dimorphism among the carnivoran species studied may influence the generalizability of the patterns identified herein based on male specimens.

RESOURCE AVAILABILITY

Lead contact

Requests for further information and resources should be directed to and will be fulfilled by the lead contact, Z. Jack Tseng (zjt@berkeley.edu).

Materials availability

This study did not generate new unique reagents.

Data and code availability

- All data reported in this paper will be shared by the lead contact upon request.
- All original code is available in this paper's supplemental information (Data S1).
- Any additional information required to reanalyze the data reported in this paper is available from the lead contact upon request.

ACKNOWLEDGMENTS

We thank Morgan Chase and the AMNH Microscopy and Imaging Facility for assistance with CT data collection. Curators and managers of the AMNH Mammalogy collections facilitated loans of the specimens used in the study. Sharlene Santana, Chris Law, and other members of the Santana Lab provided constructive feedback in earlier stages of this work. The editor, an anonymous reviewer, and reviewer David Polly provided thoughtful and highly constructive feedback that improved the statistical and methodological strength of this study. Funding for this project was provided by NSF DEB-1257572 (J.J.F., C.G., Z.J.T., and B.D.), AMNH Frick Postdoctoral Fellowship (C.G. and Z.J.T.), DBI-2128146 (Z.J.T.).

AUTHOR CONTRIBUTIONS

Conceptualization, Z.J.T. and J.J.F.; methodology, Z.J.T., C.G., and J.J.F.; investigation, Z.J.T., C.G., J.J.F., E.W., and B.D.; visualization, Z.J.T. and C.G.; supervision, Z.J.T. and J.J.F.; writing—original draft, Z.J.T. and J.J.F.; writing—review and editing, Z.J.T., C.G., J.J.F., B.D., and E.W.; funding acquisition, Z.J.T., C.G., and J.J.F.

DECLARATION OF INTERESTS

Authors declare that they have no competing interests.

STAR★METHODS

Detailed methods are provided in the online version of this paper and include the following:

- KEY RESOURCES TABLE
- EXPERIMENTAL MODEL AND STUDY PARTICIPANT DETAILS
- METHOD DETAILS
- QUANTIFICATION AND STATISTICAL ANALYSIS

SUPPLEMENTAL INFORMATION

Supplemental information can be found online at https://doi.org/10.1016/j.isci.2025.111828.

Received: August 20, 2024
Revised: November 11, 2024
Accepted: January 13, 2025
Published: January 16, 2025

REFERENCES

1. Kyomen, S., Murillo-Rincón, A.P., and Kaucká, M. (2023). Evolutionary mechanisms modulating the mammalian skull development. Philos. Trans. R. Soc. B Biol. Sci. *378*, 20220080. https://doi.org/10.1098/rstb.2022.0080.
2. Fostowicz-Frelik, Ł., and Tseng, Z.J. (2023). The mammalian skull: development, structure and function. Philos. Trans. R. Soc. Lond. B Biol. Sci. *378*, 20220077. https://doi.org/10.1098/rstb.2022.0077.
3. Koyabu, D., Werneburg, I., Morimoto, N., Zollikofer, C.P.E., Forasiepi, A.M., Endo, H., Kimura, J., Ohdachi, S.D., Truong Son, N., and Sánchez-Villagra, M.R. (2014). Mammalian skull heterochrony reveals modular evolution and a link between cranial development and brain size. Nat. Commun. *5*, 3625. https://doi.org/10.1038/ncomms4625.
4. Piekarski, N., Gross, J.B., and Hanken, J. (2014). Evolutionary innovation and conservation in the embryonic derivation of the vertebrate skull. Nat. Commun. *5*, 5661. https://doi.org/10.1038/ncomms6661.
5. Goswami, A. (2006). Cranial Modularity Shifts during Mammalian Evolution. Am. Nat. *168*, 270–280. https://doi.org/10.1086/505758.
6. Goswami, A., and Polly, P.D. (2010). The Influence of Modularity on Cranial Morphological Disparity in Carnivora and Primates (Mammalia). PLoS One *5*, e9517. https://doi.org/10.1371/journal.pone.0009517.
7. Felice, R.N., Randau, M., and Goswami, A. (2018). A fly in a tube: Macroevolutionary expectations for integrated phenotypes. Evolution *72*, 2580–2594. https://doi.org/10.1111/evo.13608.
8. Michaud, M., Veron, G., and Fabre, A.-C. (2020). Phenotypic integration in feliform carnivores: Covariation patterns and disparity in hypercarnivores versus generalists. Evolution *74*, 2681–2702. https://doi.org/10.1111/evo.14112.
9. Law, C.J., Blackwell, E.A., Curtis, A.A., Dickinson, E., Hartstone-Rose, A., and Santana, S.E. (2022). Decoupled evolution of the cranium and mandible in carnivoran mammals. Evolution *76*, 2959–2974. https://doi.org/10.1111/evo.14578.
10. Wisniewski, A.L., Nations, J.A., and Slater, G.J. (2023). Bayesian Prediction of Multivariate Ecology from Phenotypic Data Yields New Insights into the Diets of Extant and Extinct Taxa. Am. Nat. *202*, 192–215. https://doi.org/10.1086/725055.
11. Denton, J.S.S., and Adams, D.C. (2015). A new phylogenetic test for comparing multiple high-dimensional evolutionary rates suggests interplay of evolutionary rates and modularity in lanternfishes (Myctophiformes; Myctophidae). Evolution *69*, 2425–2440.
12. Blois, J.L., and Hadly, E.A. (2009). Mammalian response to Cenozoic climatic change. Annu. Rev. Earth Planet Sci. *37*, 181–208. https://doi.org/10.1146/annurev.earth.031208.100055.
13. Sansalone, G., Wroe, S., Coates, G., Attard, M.R.G., and Fruciano, C. (2024). Unexpectedly uneven distribution of functional trade-offs explains cranial morphological diversity in carnivores. Nat. Commun. *15*, 3275. https://doi.org/10.1038/s41467-024-47620-x.
14. Holliday, J.A., and Steppan, S.J. (2004). Evolution of hypercarnivory: the effect of specialization on morphological and taxonomic diversity. Paleobiology *30*, 108–128. https://doi.org/10.1666/0094-8373(2004)030<0108:EOHTEO>2.0.CO;2.

15. Badyaev, A.V., Foresman, K.R., and Young, R.L. (2005). Evolution of Morphological Integration: Developmental Accommodation of Stress-Induced Variation. Am. Nat. *166*, 382–395. https://doi.org/10.1086/432559.

16. Monteiro, L.R., and Nogueira, M.R. (2010). Adaptive radiations, ecological specialization, and the evolutionary integation of complex morphological structures. Evolution *64*, 724–744. https://doi.org/10.1111/j.1558-5646.2009.00857.x.

17. Mutumi, G.L., Hall, R.P., Hedrick, B.P., Yohe, L.R., Sadier, A., Davies, K.T.J., Rossiter, S.J., Sears, K.E., Dávalos, L.M., and Dumont, E.R. (2023). Disentangling Mechanical and Sensory Modules in the Radiation of Noctilionoid Bats. Am. Nat. *202*, 216–230. https://doi.org/10.1086/725368.

18. Wright, S. (1932). The roles of mutation, inbreeding, crossbreeding, and selection in evolution. In Proceedings of the Sixth International Congress of Genetics, pp. 356–366.

19. Simpson, G.G. (1984). Tempo and Mode in Evolution (Columbia University Press).

20. Arnold, S.J. (2003). Performance Surfaces and Adaptive Landscapes1. Integr. Comp. Biol. *43*, 367–375. https://doi.org/10.1093/icb/43.3.367.

21. Polly, P.D., Lawing, A.M., Eronen, J.T., and Schnitzler, J. (2016). Processes of ecometric patterning: modelling functional traits, environments, and clade dynamics in deep time. Biol. J. Linn. Soc. *118*, 39–63. https://doi.org/10.1111/bij.12716.

22. Tseng, Z.J., and Flynn, J.J. (2018). Structure-function covariation with nonfeeding ecological variables influences evolution of feeding specialization in Carnivora. Sci. Adv. *4*, eaao5441. https://doi.org/10.1126/sciadv.aao5441.

23. Waldman, E., Gonzalez, Y., Flynn, J.J., and Tseng, Z.J. (2023). Dental topographic proxies for ecological characteristics in carnivoran mammals. J. Anat. *242*, 627–641. https://doi.org/10.1111/joa.13806.

24. Winchester, J.M. (2016). MorphoTester: An Open Source Application for Morphological Topographic Analysis. PLoS One *11*, e0147649. https://doi.org/10.1371/journal.pone.0147649.

25. Jones, K.E., Bielby, J., Cardillo, M., Fritz, S.A., O'Dell, J., Orme, C.D.L., Safi, K., Sechrest, W., Boakes, E.H., Carbone, C., et al. (2009). PanTHERIA: a species-level database of life history, ecology, and geography of extant and recently extinct mammals: Ecological Archives E090-184. Ecology *90*, 2648. https://doi.org/10.1890/08-1494.1.

26. Baken, E.K., Collyer, M.L., Kaliontzopoulou, A., and Adams, D.C. (2021). geomorph v4.0 and gmShiny: enhanced analytics and a new graphical interface for a comprehensive morphometric experience. Methods Ecol. Evol. *12*, 2355–2363. https://doi.org/10.1111/2041-210X.13723.

27. Berthaume, M.A., Winchester, J., and Kupczik, K. (2019). Effects of cropping, smoothing, triangle count, and mesh resolution on 6 dental topographic metrics. PLoS One *14*, e0216229. https://doi.org/10.1371/journal.pone.0216229.

28. Pampush, J.D., Winchester, J.M., Morse, P.E., Vining, A.Q., Boyer, D.M., and Kay, R.F. (2016). Introducing molaR: a New R Package for Quantitative Topographic Analysis of Teeth (and Other Topographic Surfaces). J. Mamm. Evol. *23*, 397–412. https://doi.org/10.1007/s10914-016-9326-0.

29. Pampush, J.D., Crowell, J., Karme, A., Macrae, S.A., Kay, R.F., and Ungar, P.S. (2019). Technical note: Comparing dental topography software using platyrrhine molars. Am. J. Phys. Anthropol. *169*, 179–185. https://doi.org/10.1002/ajpa.23797.

30. Grohé, C., Tseng, Z.J., Lebrun, R., Boistel, R., and Flynn, J.J. (2016). Bony labyrinth shape variation in extant Carnivora: a case study of Musteloidea. J. Anat. *228*, 366–383. https://doi.org/10.1111/joa.12421.

31. Kumar, S., Suleski, M., Craig, J.M., Kasprowicz, A.E., Sanderford, M., Li, M., Stecher, G., and Hedges, S.B. (2022). TimeTree 5: An Expanded Resource for Species Divergence Times. Mol. Biol. Evol. *39*, msac174. https://doi.org/10.1093/molbev/msac174.

32. Adams, D.C., and Collyer, M.L. (2018). Multivariate Phylogenetic Comparative Methods: Evaluations, Comparisons, and Recommendations. Syst. Biol. *67*, 14–31. https://doi.org/10.1093/sysbio/syx055.

33. Esteve-Altava, B., and Rasskin-Gutman, D. (2018). Anatomical Network Analysis in Evo-Devo. In Evolutionary Developmental Biology: A Reference Guide, L. Nuno de la Rosa and G. Müller, eds. (Springer), pp. 1–19. https://doi.org/10.1007/978-3-319-33038-9_57-1.

34. Hildebrand, M., Goslow, G.E., and Hildebrand, V. (1995). Analysis of Vertebrate Structure (New York: Wiley).

35. Davis, D.D. (1964). The giant panda : a morphological study of evolutionary mechanisms. Fieldiana *3*, 1–339.

36. Finarelli, J.A., and Flynn, J.J. (2009). Brain-size evolution and sociality in Carnivora. Proc. Natl. Acad. Sci. USA *106*, 9345–9349.

37. Finarelli, J.A., and Goswami, A. (2009). The evolution of orbit orientation and encephalization in the Carnivora (Mammalia). J. Anat. *214*, 671–678. https://doi.org/10.1111/j.1469-7580.2009.01061.x.

38. Van Valkenburgh, B., Pang, B., Bird, D., Curtis, A., Yee, K., Wysocki, C., and Craven, B.A. (2014). Respiratory and olfactory turbinals in feliform and caniform carnivorans: the influence of snout length. Anat. Rec. *297*, 2065–2079. https://doi.org/10.1002/ar.23026.

39. Chung, N.C., Miasojedow, B., Startek, M., and Gambin, A. (2019). Jaccard/Tanimoto similarity test and estimation methods for biological presence-absence data. BMC Bioinf. *20*, 644. https://doi.org/10.1186/s12859-019-3118-5.

40. Gingerich, P.D. (1993). Quantification and comparison of evolutionary rates. Am. J. Sci. *293*, 453–478. https://doi.org/10.2475/ajs.293.A.453.

41. Polly, P.D. (2001). Paleontology and the comparative method: ancestral node reconstructions versus observed node values. Am. Nat. *157*, 596–609. https://doi.org/10.1086/320622.

STAR★METHODS

KEY RESOURCES TABLE

REAGENT or RESOURCE	SOURCE	IDENTIFIER
Deposited data		
Cranial shape data	Tseng and Flynn[22]	https://doi.org/10.1126/sciadv.aao5441
Dental topographic data	Waldman et al., [23]	https://doi.org/10.1111/joa.13806
Software and algorithms		
Geomorph R Package	https://cran.r-project.org/web/packages/geomorph/index.html	Version 4.0.9.
Jaccard R Package	https://cran.r-project.org/web/packages/jaccard/index.html	Version 0.1.0.
Morphotester	Winchester[24]	https://doi.org/10.1371/journal.pone.0147649 Version 1.0.1
Phylogenetic tree	timetree.org	Accessed December 2023.
PanTHERIA trait database	Jones et al.[25]	https://esapubs.org/archive/ecol/E090/184/
R script	This study (as supplemental information)	Data S1

EXPERIMENTAL MODEL AND STUDY PARTICIPANT DETAILS

Skull specimens of 29 carnivoran species were included in this study. All specimens came from the Mammalogy (prefix M) or Vertebrate Paleontology (prefix VP) collections of the American Museum of Natural History. Adult male specimens were selected based on full eruption of the permanent dentition and sex information recorded in the collections database. The specimens used were: *Acinonyx jubatus* (VP CA2502), *Ailuropoda melanoleuca* (M89079), *Arctonyx collaris* (M57373), *Bassariscus astutus* (M135964), *Callorhinus ursinus* (M71169), *Cryptoprocta ferox* (M100463), *Eira Barbara* (M32065), *Enhydra lutris* (M24186), *Erignathus barbatus* (M98), *Fossa fossa* (M188210), *Hydrurga leptonyx* (M34920), *Lutra lutra* (M206592), *Lycaon pictus* (VP24218), *Mellivora capensis* (M89011), *Mephitis mephitis* (M172133), *Mustela frenata* (M60508), *Mydaus javanensis* (M106635), *Nandinia binotata* (M51452), *Odobenus rosmarus* (M19270), *Panthera pardus* (M113745), *Phoca vitulina* (M100), *Potos flavus* (M239990), *Procyon lotor* (M24815), *Spilogale putorius* (M35207), *Taxidea taxus* (M120577), *Tremarctos ornatus* (M99308), *Ursus arctos* (M34408), *Vulpes vulpes* (M88713), and *Zalophus californianus* (M63946).

METHOD DETAILS

We collected or compiled geometric morphometric shape data and dental topographic data from the cranium, mandible, and dentition of 29 extant carnivoran mammal species. The cranial shape data come from,[22] the dental topographic data come from,[23] and the mandibular and inner ear bony labyrinth shape data were collected from digital models built using CT scan data.

*Cranial shape data (*Figure 1G*)*—74 fixed landmarks and 116 semi-landmarks from[22] were extracted for those of the 29 species that also are sampled for the three other data partitions. We aligned the landmark dataset and removed effects of rotation, translation, and isometric size using the generalized Procrustes superimposition method, implemented in the Geomorph package in the R programming environment.[26]

*Dental topographic data (*Figure 1F*)*—The postcanine dental topographic data from[23] were trimmed to mirror the 29 taxa matching carnivoran mammal species in the other comparative studies herein. We used three topographic characteristics summarizing the lower left postcanine tooth crown surface to characterize dental topography: (1) Dirichlet normal energy (DNE), (2) orientation patch count rotated (OPCR), and (3) relief index (RFI). Dental surface area was compared across samples to standardize resolution of micro-computed tomography (μCT) voxel size. The postcanine dentition was cropped according to the methods in Berthaume et al.[27] to compare the entire enamel cap (EEC) cropping method among the analyzed species. Measurements of DNE, OPCR, and RFI were calculated in MorphoTester 1.0.1 software.[24] Mesh sensitivity of postcanine dental topographic surfaces among species were standardized for both highest and lowest resolution scans, using established methods in prior studies.[28,29]

*Mandibular shape data (*Figure 1E*)*—We collected 57 three-dimensional fixed landmarks and semilandmarks on 3-D polygon meshes of carnivoran hemimandibles. We used the dentition as a reference for placing some of the landmarks, but no shape data were collected directly from tooth crowns. Therefore, this dataset represents mandibular body shape only. We aligned the landmark

dataset and removed effects of rotation, translation, and isometric size using the generalized Procrustes superimposition method, implemented in the Geomorph package in the R programming environment, as for the cranial landmark dataset.

*Bony labyrinth shape data (*Figure 1D*)*—We collected 126 fixed and semilandmarks on 3-D models of the bony labyrinth (inner ear cochlea + semicircular canals) in the 29 taxa using the methodology in.[30] We aligned the landmark dataset and removed effects of rotation, translation, and isometric size using the generalized Procrustes superimposition method, implemented in the Geomorph package in the R programming environment, as for the cranial landmark dataset.

Morphological modules—We categorized the datasets described above into 9 different morphological modules. First, we coded all cranial landmarks and semilandmarks into one of six morphological modules previously identified in mammal skulls by Goswami and Polly.[6] These modules included: (1) anterior oral & nasal, (2) orbit, (3) cranial vault, (4) palate, (5) zygomatic-pterygoid, and (6) basicranium regions. The remaining, new data partitions were kept as individual modules for their unique developmental origins and osteological distinctiveness: (7) mandibular body (''mandible''), (8) dental topography (''dentition''), and (9) bony labyrinth (''ear'').

Phylogeny—We used a phylogeny pruned to the 29 taxa present across all data partitions from timetree.org,[31] to incorporate phylogenetic information in our comparative analyses. Branch lengths of the phylogeny are based on molecular divergence times (Figure 2).

Ecological categories—We analyzed three ecological traits against the network models: 1) dietary breadth, 2) habitat breadth, and 3) terrestriality (Figure 2). These traits were chosen for their relevance to masticatory (dietary breadth) and sensory (habitat breadth/complexity, and dimensionality/terrestriality of the environment each taxon lives in) functions performed by the skull. Trait values for each sample taxon were extracted from the PanTHERIA database,[25] with the following definitions from that database:

1) Dietary breadth: ''Number of dietary categories eaten by each species measured using any qualitative or quantitative dietary measure, over any period of time, using any assessment method, for non-captive or non-provisioned populations; adult or age unspecified individuals, male, female, or sex unspecified individuals; primary, secondary, or extrapolated sources; all measures of central tendency; in all localities. Categories were defined as vertebrate, invertebrate, fruit, flowers/nectar/pollen, leaves/branches/bark, seeds, grass and roots/tubers.''[25]
2) Habitat breadth: ''Number of habitat layers used by each species measured using any qualitative or quantitative time measure, for non-captive or non-provisioned populations; adult or age unspecified individuals, male, female, or sex unspecified individuals; primary, secondary, or extrapolated sources; all measures of central tendency; in all localities. Categories were defined as above ground dwelling, aquatic, fossorial and ground dwelling.''[25]
3) Terrestriality: ''Degree of terrestriality of each species measured using any qualitative or quantitative time measure, for non-captive or non-provisioned populations; adult or age unspecified individuals, male, female, or sex unspecified individuals; primary, secondary, or extrapolated sources; all measures of central tendency; in all localities. Species were defined as (1) fossorial and/or ground dwelling only and (2) above ground dwelling''.[25] In addition to analyses using this two-category scheme, sensitivity analyses were conducted by splitting the first category (fossorial and/or ground dwelling only) into non-aquatic terrestrial (terra1) versus semi-aquatic/aquatic (terra3) taxa, in addition to the above ground dwelling taxa (terra2).

Because the PanTHERIA database trait variable definitions were based on trait distributions across all mammals, and the current study examines only carnivorans, several modifications were made to simplify the categories of each ecological trait to enable more samples within each category. Mixed dietary breadth with intermediate scores of 2 to 5 were all coded as 3, so a given taxon had either 1 (specialists), 3 (a broad range of mixed dietary breadth), or 6 (generalists) as their dietary breadth score. Habitat breadth score 2 and 3 (occupying two or three habitats out of the four habitat categories: above ground dwelling, aquatic, fossorial and ground dwelling) were binned because only one sampled carnivoran exhibited a score of 3. Lastly, the sea otter was coded with a terrestriality score of 1 (*not* above ground dwelling) to be included in the core analyses and coded as terra3 in the sensitivity analyses.

QUANTIFICATION AND STATISTICAL ANALYSIS

Integration tests and model testing—We assessed the presence of potential second-order phenotypic module networks linking some of the nine first-order modules by using both 1) phylogenetic integration tests under a Brownian motion model with no *a priori* integrated module definition (referred to as the baseline carnivoran model) and 2) a network-similarity based test with three predefined second-order network models (topological, masticatory, and sensory models; Figures 1A–1C). We quantified pairwise covariation between the nine morphological modules using partial least squares (PLS) correlation that takes phylogeny into account, applying a Brownian motion model. We then tested for statistical significance of the covariations using permutation tests, implemented in the *phylo.integration* function of the Geomorph package.[32] This phylogenetic integration test was performed on the entire dataset of the 9 data partitions.

In addition to phylogenetic integration tests, we defined and tested support for three different *a priori* models of expected higher-level organization of the common mammal skull modules. These three models respectively represent module covariation patterns that follow a (1) topology-driven module proximity regime, (2) masticatory function-driven regime, or (3) sensory function-driven regime (Table 1; Figures 1A–1C). The topological network model is one where adjacent/contiguous morphological modules covary, but non-adjacent morphological modules do not covary. The definition of this model is similar to the concept of anatomical network analysis proposed by Esteve-Altava et al.[33] The masticatory network model is one where the cranial vault, palate, zygomatic-pterygoid, dental topography, and mandible shape modules exhibit significant covariation with each other because of their participation in the origination and attachment of jaw-closing musculature and/or mastication.[34] The sensory network model is one where the basicranium, cranial vault, bony labyrinth, orbit, and anterior oral and nasal regions exhibit significant covariation with each other because of their participation in housing portions of the central nervous system and/or special sensory organs (e.g., olfactory, auditory, visual, taste). Given that the sensory system is principally soft tissue-based, we do not necessarily expect its surrounding bone tissue to reflect nuanced functional differences in those senses. Nevertheless, shape changes in the basicranium, which broadly captures nerve entrances for several of the special senses (e.g.,[35]); the cranial vault, which has been used as a proxy for encephalization and brain processing capability across carnivorans[36]; the bony labyrinth, which correlates with locomotor modes through the control of balance[30]; the orbit, which may indicate visual field depth and breadth,[37] and the rostral region, whose external shape may correlate with the volume and size of turbinate bones involved in respiration and olfaction,[38] all may still retain general information about sensory adaptation trends across the order-level carnivoran dataset we chose as our study system.

Finally, for data partitions of ecological categories, a fourth network model represented by the linkage relationships of the full dataset was tested against network linkages generated by each data partition. Goodness of fit of the four network models to the carnivoran skull dataset was assessed using the Jaccard similarity index, which is calculated as the ratio between the intersecting network nodes between two networks and the total number of unique nodes in the network. Statistical significance of the calculated Jaccard similarity index was assessed using both a bootstrap and an exact method, both implemented in the Jaccard package in R.[39]

Evolutionary rate comparisons—in addition to testing the mode of skull phenotypic network connectivity among skull regions, we also compared patterns of covariation in evolutionary rates among the first-order morphological modules. The predefined topological, sensory, and masticatory network models were used to subset the carnivoran phenotypic dataset, and evolutionary rates then were calculated and compared across the categories within each ecological trait based on a Brownian motion model of evolution. Permutation tests were then used to assess the statistical significance of rate differences between ecological categories. The rate comparisons and tests were run using the *compare.evol.rates* function from the Geomorph R package.[26] To maximize the contribution of module-specific morphological change to evolutionary rate estimation (and to minimize the potential effect of correlated shape changes among first order modules), Procrustes superimpositions of the trait data used for rate estimation were performed separately for each morphological module rather than as a single shape configuration. The calculation of evolutionary rates is accordingly adjusted in the rate equation based on.[11]

Our preliminary analyses of evolutionary rates based on superimposed (landmark-based) and raw (dental topographic indices) trait data indicated the presence of several orders of magnitude difference in estimated rates. The evolutionary rates of dental topographic traits are always much higher than those of landmark-based morphological traits. To correct for the influence of different units of measurement between landmark and dental data, and also between landmark-based data partitions that contain different quantities of landmark coordinates, we scaled all traits by their pooled within-family standard deviation values.[40,41] Family-level standard deviation values were used rather than lower level within-taxon values, because only a single individual of each taxon was sampled for all first-order module trait data for this study. All subsequent estimates of evolutionary rates were performed using the scaled trait deviate values.

Sampling power—Given the relatively small number of taxa sampled (29 species), we replicated a series of network module analyses using simulated data to estimate the statistical probability that the observed ecological groupings represent only a random sample of network relationships rather than ones with a biological or evolutionary basis. For these analyses ,we generated and analyzed a simulated trait dataset that contained the same number of taxa (n = 29) as our empirical dataset. First, trait data for all of the first-order morphological modules were resampled by randomly selecting trait data from each data partition to generate a new simulated ‘‘taxon’’ with a random combination of morphological traits. This process was repeated without replacement so that the final, 29-taxon simulated dataset represented a randomized combination of the original empirical trait datasets. The simulated dataset was then subjected to the same phylogenetic integration tests as described above for the empirical dataset. Network edge lists and graphs were similarly generated from the phylogenetic integration results. To evaluate whether the resulting second-order network modules from randomly-generated simulated data were significantly different in their Jaccard similarity index from those determined for the empirical dataset, we calculated pairwise Jaccard similarity indices within the empirical and simulated datasets, respectively. The network modules included in these pairwise calculations were sampled from the three dietary breadth categories, two habitat breadth categories, two terrestriality categories, and the overall phylogenetic integration network. A Levene’s test of homogeneity of variance was implemented to assess the statistical significance of the difference between the empirical and simulated Jaccard indices. Lastly, the resulting distributions of pairwise Jaccard similarities were plotted as boxplots and density

plots (Figure 6). If the empirical dataset differed significantly from the simulated dataset in the distribution of Jaccard similarity indices, then the empirical dataset values were unlikely to have been sampled from the same population as the randomized simulated dataset. On the other hand, if the two datasets did not differ significantly in the distribution of Jaccard indices, then we could not exclude the possibility that any differences in the empirically sampled second-order networks may have arisen by chance, as if they were sampled from a random population.

Functions and scripts for the analyses described in this section are included as a supplemental file (Data S1).